PHYSICAL REVIEW B **86**, 100402(R) (2012)

Frustrated magnets and quantum paramagnetic phases at finite temperature

L. Isaev[1] and G. Ortiz[2]

[1]*Department of Physics and Astronomy, Louisiana State University, Baton Rouge, Louisiana 80703, USA*

[2]*Department of Physics and Center for Exploration of Energy and Matter, Indiana University, Bloomington, Indiana 47405, USA*

(Received 11 April 2012; revised manuscript received 29 May 2012; published 12 September 2012)

We develop a general framework, which combines exact diagonalization in small clusters with a density matrix variational principle, to study frustrated magnets at finite temperature. This thermodynamic hierarchical mean-field technique is used to determine the phase diagram and magnetization process of the three-dimensional spin-1/2 J_1-J_2 antiferromagnet on a stacked square lattice. Its nonmagnetic phase exhibits a thermal crossover from a quantum to a classical paramagnet at a temperature $T = T_0$ which can be extracted from thermodynamic measurements. At low temperature an applied magnetic field stabilizes, through order by disorder, a variety of phases with nontrivial spin textures, and a magnetization plateau at half-saturation which continuously disappears at $T \sim T_0$. Our results are relevant for frustrated vanadium oxides.

DOI: 10.1103/PhysRevB.86.100402 PACS number(s): 75.10.Jm, 75.10.Kt, 75.40.Cx, 75.60.Ej

Introduction. Frustrated magnetic materials have been the focus of active condensed matter research in the past two decades.[1] In these systems, competing interactions and frustrated lattice topology often lead to fascinating effects, e.g., magnetic monopoles[2,3] in spin ice materials or magnetization plateaus in an applied magnetic field,[4,5] and stabilize exotic quantum states of matter, such as spin liquids[6] or valence bond solids.[7] Understanding these paramagnetic phases, which do not break any obvious global symmetry and thus are not necessarily identified by an order parameter, is of fundamental interest in material physics.

The theoretical description of frustration-driven phenomena is extremely challenging, especially in spatial dimensions larger than one. For example, frustrating interactions render large-scale quantum Monte-Carlo (QMC) simulations impractical due to the "sign problem."[8] Various approaches were developed to tackle frustrated magnets.[9] One class of methods proposes an expansion around a magnetically ordered state (spin-wave and series expansions), or in certain limiting cases, e.g., high temperature. Another class focuses on ground state (GS) properties of the system (coupled cluster and Lanczos methods). Meanwhile it is both theoretically and experimentally[6] relevant to inquire: What are the potential signatures of magnetic frustration in the thermodynamic properties of a given material? Clearly, quantum effects due to a nontrivial GS will become apparent at temperatures of the order of the characteristic energy scales involved in the formation of that particular GS.

In the present Rapid Communication we address the above question. We develop an unbiased and general framework aimed at studying the interplay between quantum and thermal fluctuations in frustrated magnets. Our method couples the recently developed hierarchical mean-field (HMF) theory[10] and the well-known thermodynamic variational principle.[11] A key idea is the realization that various competing *local* orders can only be captured within an *exact diagonalization* scheme, while transitions between them will be correctly described only in an *infinite* system. Hence, one starts by partitioning a lattice into relatively small spin clusters (degrees of freedom) in accordance with point-group symmetries. These new degrees of freedom provide a language in which the original model Hamiltonian is represented. Approximations are introduced in the form of a variational principle applied to the free energy in the new representation. Our approach relies on numerical as well as analytical efforts: Provided the cluster is chosen properly, even a simple variational ansatz for the density matrix (DM) yields a *complete* phase diagram of the system. Results can be systematically improved by considering larger clusters or more complicated trial DMs. Once the system DM is known, any observable can be computed even *inside* nonmagnetic (paramagnetic) phases, in contrast to the usual mean-field (MF) techniques which only yield instabilities of the magnetically ordered states.

We illustrate the thermodynamic HMF (THMF) formalism by studying the phase diagram at finite temperature T and properties in an applied magnetic field of the "stacked" J_1-J_2 model,[12–14] which describes a spin-1/2 Heisenberg antiferromagnet on an orthorhombic lattice with first (J_1) and second (J_2) neighbor interactions in the ab-plane, and a nearest-neighbor (NN) exchange (J_C) along the c-axis. This model is a good approximation for layered vanadium oxide materials,[15–17] such as $Li_2VO(Si,Ge)O_4$ (Ref. 18) and $PbVO_3$.[19] Previous works indicate that at $T = 0$ the J_1-J_2-J_C model exhibits a quantum paramagnetic phase whose stability can be controlled by changing J_C. We show that this phase persists even at finite T and introduce an important temperature scale T_0 at which a crossover from quantum to classical paramagnetic behavior takes place. The numerical value of T_0 can be extracted from thermodynamic or magnetization measurements. Below T_0, an interplay between quantum fluctuations inside the paramagnetic region and external field results in a variety of phases characterized by nontrivial magnetic orders, and leads to a magnetization plateau around half of the saturation field. Our findings are directly relevant for the frustrated perovskite $PbVO_3$, which shows no magnetic order and is believed to realize a J_1-J_2 quantum paramagnet.[19]

The THMF method. Let us consider a quantum spin model defined on a lattice with N sites and periodic boundary conditions. Following the HMF prescription,[10] we partition the lattice into $N_\square$ clusters of N_q sites each, so that $N = N_\square N_q$. It is assumed that eigenstates of an isolated cluster are known. Each cluster state $|a\rangle$ can be associated with a Schwinger

boson $\gamma_a^\dagger$, subject to a constraint $\sum_a \gamma_a^\dagger \gamma_a = 1$. It is important to note that the version of the THMF method developed below treats this constraint *exactly*, a condition that is crucial for the method to be variational.

In terms of "cluster" degrees of freedom the original Hamiltonian of the system can be written as

$$H = \sum_i (H_0)_{ab} \gamma_{ia}^\dagger \gamma_{ib} + \sum_{ij} (V_{ij})_{ab}^{a'b'} \gamma_{ia'}^\dagger \gamma_{jb'}^\dagger \gamma_{jb} \gamma_{ia}, \qquad (1)$$

with H_0 and V being the cluster self-energy and intercluster interaction, respectively. The subscript i labels different clusters in the coarse-grained lattice and summation over doubly repeated indices is assumed. The range and type of couplings in the second term are determined by the original model. Each spin (and therefore each cluster) has ν_λ links of type λ ($\lambda = 1,2,\ldots$) with corresponding interactions V_λ. For instance, on a square J_1-J_2 lattice there are $\nu_1 = 2$ NN and $\nu_2 = 2$ next-NN (NNN) links per site. The Hamiltonian (1) operates on a Hilbert space spanned by the products $|\{a\}\rangle = \prod_i \gamma_{ia_i}^\dagger |0\rangle$, where $|0\rangle$ is the unphysical Schwinger boson vacuum corresponding to all "empty" clusters.

The THMF theory is a variational approach with respect to the free energy. Here we consider a simple trial DM, $\rho_0[H_{\rm MF}] = e^{-K/T}/Z_0$, with $K = \sum_i (H_{\rm MF})_{ab} \gamma_{ia}^\dagger \gamma_{ib}$, where the Boltzmann constant $k_B \equiv 1$, and the MF Hamiltonian $H_{\rm MF}$, whose matrix elements play the role of variational parameters,[11] is self-consistently determined by minimizing the free energy $F = E - TS = {\rm Tr}\,\rho_0(H + T\ln\rho_0) = {\rm Tr}\,\rho_0(H - K) - T\ln Z_0$. The partition function can be expressed in terms of the eigenvalues E_n of $H_{\rm MF}$ as $Z_0 = Z_1^{N_\square}$ with $Z_1 = \sum_n e^{-E_n/T}$. Then the free energy becomes

$$\frac{F}{N_\square} = -T\log Z_1 + {\rm tr}_1\omega_1 \left[H_0 + \sum_\lambda \nu_\lambda {\rm tr}_2 (V_\lambda)_{12}\omega_2 - H_{\rm MF} \right].$$

Here $\omega = e^{-H_{\rm MF}/T}/Z_1$ is the single-cluster DM, "tr" denotes a trace over single-cluster MF states, and ${\rm tr}_1{\rm tr}_2(V_\lambda)_{12}\omega_1\omega_2 = (V_\lambda)_{a_1a_2}^{a_1'a_2'}\omega_{a_1a_1'}\omega_{a_2a_2'}$.

A simple calculation yields the MF Hamiltonian[11]

$$(H_{\rm MF})_{a'a} = (H_0)_{a'a} + 2\sum_\lambda \nu_\lambda (V_\lambda)_{ab_2}^{a'b_1}\omega_{b_2b_1}. \qquad (2)$$

Using its eigenstates R_a^n one can compute the DM ω:

$$\omega_{ab} = \sum_n e^{-E_n/T} R_a^n \left(R_b^n\right)^* \Big/ \sum_n e^{-E_n/T} \qquad (3)$$

and the free energy $F/N = (1/2N_q){\rm Tr}\,\omega(H_0 - H_{\rm MF}) - (T/N_q)\ln Z_1$. In the limit $T \to 0$ only the GS eigenpair (E_0, R^0) contributes to the DM (3), i.e., $\omega_{ab} \to R_a^0 (R_b^0)^*$, and we recover the $T = 0$ HMF results.[10]

Expressions (2) and (3) define the THMF self-consistent (in terms of ω_{ab}) scheme. Any local observable $\langle O\rangle$ can be computed as $\langle O\rangle = {\rm tr}\,\omega O$.

J_1-J_2-J_C model. We now use the THMF method to study the J_1-J_2-J_C model[12] (Fig. 1):

$$H = \left(J_1 \sum_{\langle ij\rangle} + J_2 \sum_{\langle\langle ij\rangle\rangle} + J_C \sum_{\langle ij\rangle_z} \right) \boldsymbol{S}_i \boldsymbol{S}_j - h\sum_i S_i^z, \qquad (4)$$

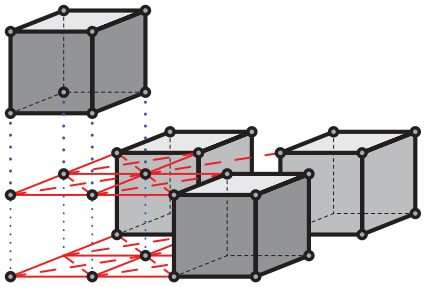

FIG. 1. (Color online) The J_1-J_2-J_C lattice. Solid, dashed, and dotted lines denote J_1, J_2, and J_C exchange interactions, respectively. Shaded cubes are clusters used in the THMF calculation.

where all couplings $J_{1,2,C}$ are positive, $\boldsymbol{S}_i$ is a spin-1/2 operator at site i, and h is an external magnetic field. This model describes a three-dimensional (3D) analog of the J_1-J_2 antiferromagnet[20] defined on a cubic lattice with intralayer NN ($\langle ij\rangle$) and NNN ($\langle\langle ij\rangle\rangle$) interactions J_1 and J_2, respectively, and an interlayer NN ($\langle ij\rangle_z$) exchange J_C. In the following we adopt the units $J_1 \equiv 1$.

At $h = T = 0$, the coupling J_C can be viewed as a tuning parameter controlling quantum effects associated with frustration. In particular, for $J_C > J_C^0$ the quantum paramagnetic phase of the J_1-J_2 model disappears and the system exhibits a direct first-order transition from Néel to a columnar antiferromagnetic (AF) state. For $J_C < J_C^0$ there is an intermediate nonmagnetic region which appears for a finite range of J_2 and vanishes at J_C^0. Thus the point $[J_2(J_C^0), J_C^0]$ is a multicritical point where three phase boundaries converge. There seems to be a controversy regarding the order of phase transitions occurring at these boundaries: Spin-wave studies[13] predict one second- and two first-order lines, while series expansions[14] indicate that all phase boundaries are first order. Our analysis supports the spin-wave scenario.[21]

We apply the THMF theory to compute the finite-temperature phase diagram of Hamiltonian (4). While the effect of thermal fluctuations on ordered phases is well known, their role inside a *quantum* nonmagnetic state is unclear. Since this state does not break any continuous symmetry, the system can only undergo a crossover from a quantum to a standard classical paramagnet. We will show how the corresponding temperature scale can be deduced from experimentally accessible thermodynamic quantities, such as specific heat or uniform susceptibility. We also study properties of the J_1-J_2-J_C model in an applied magnetic field. In the paramagnetic phase the magnetization curve has a plateau, similar to that of Ref. 22 obtained for the two-dimensional (2D) J_1-J_2 model at $T = 0$. We demonstrate that with increasing field, a system exhibits a set of metamagnetic transitions characterized by noncoplanar spin textures.

Application of the THMF technique starts by selecting a proper degree of freedom. Since the J_1-J_2-J_C lattice has an orthorhombic unit cell with symmetry D_{2h},[23] the smallest cluster compatible with this symmetry is a cube, shown in Fig. 1. Each cluster has six NN (four in the ab-plane, two along the c-axis) and four NNN clusters in the ab plane; i.e., $\nu_1 = \nu_2 = 2$ and $\nu_C = 1$ in Eq. (2). Next, we compute the matrices H_0 and V in Eqs. (1) and (2) using the method of

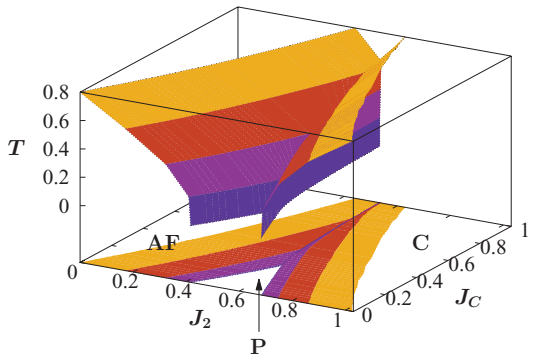

FIG. 2. (Color online) Phase diagram of the J_1-J_2-J_C model at $h = 0$ ($J_1 = 1$). There are three phases: (π,π,π)-Néel antiferromagnet (AF), $(0,\pi,\pi)$-columnar AF (C), and paramagnet (P).

Ref. 10. Finally, ω_{ab} is determined self-consistently using Eqs. (2) and (3).

Finite-T phase diagram. The zero-field phase diagram of the J_1-J_2-J_C model (4) is presented in Fig. 2. At $T = 0$ and $J_C < J_C^0$ there exist three phases: AF with the wave vector $\boldsymbol{Q} = (\pi,\pi,\pi)$, plaquette quantum paramagnet (P), and columnar AF (C) with $\boldsymbol{Q} = (0,\pi,\pi)$ or $(\pi,0,\pi)$. The magnetic phases are characterized by an order parameter of the form $M_i = \langle \boldsymbol{S}_i \rangle = M_{\boldsymbol{Q}} e^{i\boldsymbol{Q}\boldsymbol{x}_i}$. The transition AF-P (P-C) is second (first) order for all values of J_C. This conclusion is consistent with the phase diagram of the J_1-J_2 ($J_C = 0$) model[10] and agrees with the spin-wave[13] and coupled cluster[12] analysis. For $J_C > J_C^0$ there is only a first-order AF-C transition. The THMF calculation yields $J_C^0(T = 0) \sim 0.28$–0.30, in agreement with previous works.[12–14] The real-space structure inside the P region is *plaquette crystal-like* with layers covered with 2×2 plaquettes, each being in its singlet GS. This state is similar to the paramagnetic GS of the 2D J_1-J_2 model[10] and is stabilized because for the P-phase J_C is quite small, so the system exhibits quasi-2D behavior.

With increasing T the ordered AF and C states are suppressed via a second-order (classical) phase transition at a Néel temperature $T_N(J_2, J_C)$, which is accompanied by a jump in the magnetic specific heat C_v [see Fig. 3(a)]. Since the THMF method ignores long-range fluctuations, T_N remains finite even in the 2D limit $J_C = 0$, which constitutes a violation of the Mermin-Wagner theorem[24] common to MF theories. We note that in the C state along with the columnar magnetization M_c one can introduce an Ising order parameter[25,26]

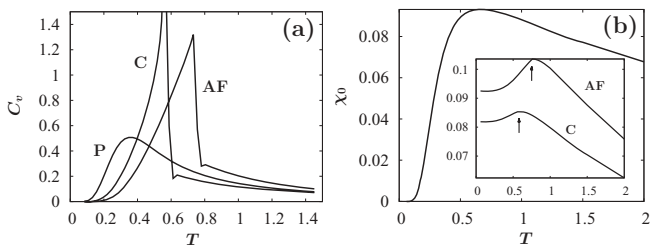

FIG. 3. (a) Specific heat C_v for the phases in Fig. 2 at $J_C = 0.1$: AF ($J_2 = 0.1$), P ($J_2 = 0.5$), and C ($J_2 = 0.8$). (b) Uniform susceptibility χ_0 for the paramagnetic phase (main plot), and magnetic states (inset) with arrows indicating the Néel temperature. Parameters are the same as in (a).

$\sigma = (1/N)\sum_{x,y} \boldsymbol{S}_{x,y}(\boldsymbol{S}_{x+1,y} - \boldsymbol{S}_{x,y+1})$, with the summation extending over N sites of the original lattice and $(x,y) \equiv i$. This $\mathbb{Z}_2$ order parameter is not subject to the conditions of the Mermin-Wagner theorem and vanishes at a nonzero temperature[25] via a second-order phase transition. However, at the HMF level σ and M_c vanish at the same Néel temperature.

Inside the P phase, a crossover takes place from quantum (at low T) to classical (at high T) behavior. Because the paramagnetic GS is gapped, C_v exhibits a peak [Fig. 3(a)]. We argue that the position of this peak serves as an estimate of the crossover temperature T_0 at which thermal fluctuations become comparable to the gap in the GS. For instance, at $J_2 = 0.5$ and $J_C = 0.1$, $T_0 \sim 0.3$. The gap in the P state manifests itself in an activated behavior of the uniform linear magnetic susceptibility $\chi_0(T) = \partial M_z/\partial h|_{h=0}$, presented in Fig. 3(b). Contrary to the ordered AF and C states where $\chi_0(T = 0)$ is finite and has a peak approximately at the corresponding T_N, for the P-phase $\chi_0(T = 0) = 0$, and shows a broad maximum around T_0. Since the P phase has a plaquette structure, it is natural to examine the behavior of various plaquette "order parameters." We considered the functions $F_4 = (1/N)\sum_{x,y} \boldsymbol{S}_{x,y}[(-1)^x \boldsymbol{S}_{x+1,y} + (-1)^y \boldsymbol{S}_{x,y+1}]$ and $Q = (1/2N)\sum(P_{1234} + P_{1234}^{-1})$ introduced in Refs. 26 and 27, respectively. In the expression for Q the summation takes place over plaquettes in ab-planes and P_{1234} is an operator of cyclic permutation of plaquette vertices. Both functions remain finite and decay as $\sim 1/T$ at large temperature. The crossover manifests itself through a peak in dF_4/dT and dQ/dT around T_0. As any real-space method, the THMF theory involves explicit translational symmetry breaking (cf. Ref. 21), predicting a crossover inside the paramagnetic phase. In an exact thermodynamic limit solution this crossover may become a phase transition because of melting of the plaquette crystal.

Now let us consider transitions between different phases, which are triggered by tuning J_2 while keeping $T > 0$ and J_C fixed. The transition AF-P remains second-order. On the other hand, the transition P-C is clearly discontinuous at low T because symmetries of the two phases are not related by the group-subgroup relation.[10] At higher T (still not destroying the magnetic order), the jump in the columnar magnetization vanishes and the transition becomes continuous.

Finally we compare the critical temperature and exponents obtained from the eight-spin cluster THMF with their known values. For the unfrustrated 3D Heisenberg model ($J_2 = 0$ and $J_C = 1$) the specific heat and order parameter exponents are $\alpha_{\mathrm{THMF}} = 0$ and $\beta_{\mathrm{THMF}} = 0.470(1)$, and the Néel temperature is $T_N^{\mathrm{THMF}} = 1.308$. These values should be compared with the results of the Weiss molecular field $\alpha_W = 0$, $\beta_W = 0.5$, $T_N^W = 1.5$, and QMC[28,29] $\beta_{\mathrm{QMC}} = 0.36$, $T_N^{\mathrm{QMC}} = 0.946$. Near the paramagnetic phase, e.g., for $J_2 = 0.3$ and $J_C = 0.1$, we have $\beta_{\mathrm{THMF}} = 0.474(2)$ and $T_N^{\mathrm{THMF}} = 0.512$. The THMF exponents and T_N can be improved by increasing the cluster size and implementing a finite-size extrapolation.

Magnetic states in an applied field. An exhaustive spin-wave study of the magnetization process $M(h)$ inside ordered phases of the J_1-J_2-J_C model was performed in Ref. 16. On the contrary, high-field properties of the quantum paramagnetic state received much less attention, with efforts exclusively

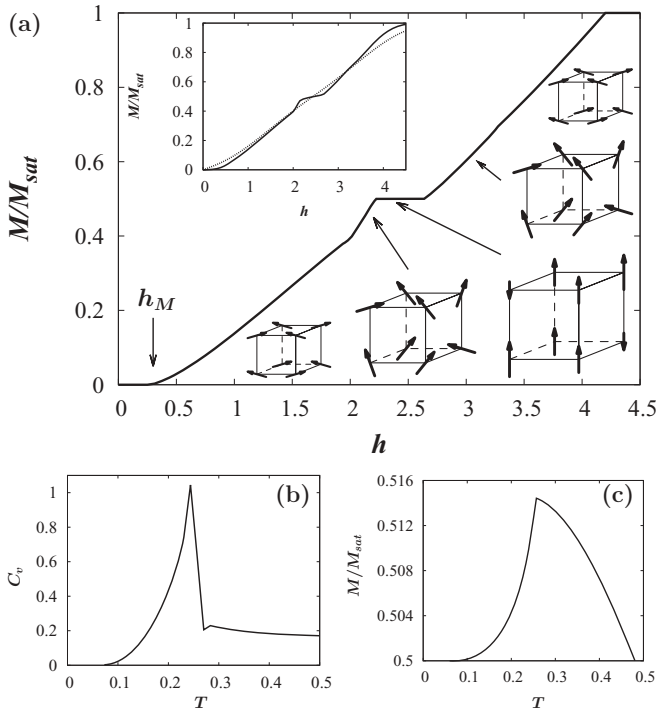

FIG. 4. (a) Magnetization process of the J_1-J_2-J_C model with $J_2 = 0.5$, $J_C = 0.1$, and $M_{\rm sat} = 1/2$. Main panel: Total magnetization M vs applied field at $T = 0$ and schematic spin profiles in the corresponding field ranges (the length of the arrows is proportional to the magnitude of the spin expectation values). Inset: M at finite temperature $T = 0.16$ (solid line) and $T = 0.3$ (dotted line). (b) and (c) Temperature dependence of the specific heat and M at $h = 2.5$. The second-order phase transition happens at $T \sim T_0$.

focused on the case $J_C = 0$ (2D J_1-J_2 model). Particularly, in Ref. 22 a half-saturation ($M = 1/4$) magnetization plateau characterized by a collinear spin ordering was proposed around the maximally frustrated point $J_2 = 0.5$.

Here we apply the THMF theory to study field-induced metamagnetic transitions inside the nonmagnetic region (Fig. 2) of the J_1-J_2-J_C model with $J_2 = 0.5$ and $J_C = 0.1$. The main panel of Fig. 4(a) displays the $T = 0$ magnetization curve. For h below certain threshold value h_M, the magnetization vanishes due to the spectral gap. For $h > h_M$, the system exhibits a set of phases with noncoplanar magnetic textures, shown in the figure. While the spin orderings at small and large fields simply reflect canted AF sublattices, the structures immediately before and after the 1/2-plateau are nontrivial because the classical canting angle varies for different spins. The plateau state has long-range order characterized by a collinear magnetic structure with two spins per cluster antiparallel to the field (cf. Ref. 22) and an Ising order parameter.

The plateau width [Fig. 4(a), inset] and threshold field h_M vanish at $T \sim T_0$, in agreement with the behavior of C_v [Fig. 3(a)]. For a fixed field inside the plateau, the magnetic order collapses via a second-order phase transition at $T \sim T_0$. In Figs. 4(b) and 4(c) we show the temperature dependence of C_v and M at $h = 2.5$. The nonmonotonic behavior of $M(T)$ is easy to understand by observing that at $T = 0$ spins are "locked" in a specific pattern by the interactions. Thermal fluctuations unlock the spins allowing them to orient along the field, thus increasing $M(T)$ before the transition. This highly nontrivial magnetization process is specific to the P state in Fig. 2, and we propose to use it in conjunction with the peak in C_v as characteristic signatures of a quantum paramagnet.

Conclusion. We developed and applied the THMF method to address the interplay between quantum and thermal fluctuations in the spin-1/2 J_1-J_2-J_C antiferromagnet. Focusing on the nonmagnetic region of the model, which is inaccessible for other theoretical techniques, we studied the crossover between a classical (due to thermal effects) and a quantum paramagnet, and demonstrated how the crossover temperature scale T_0 can be extracted from thermodynamic and high-field measurements. At low temperature $T < T_0$ quantum fluctuations inside the paramagnetic state are manifested in a variety of field-induced spin structures and a magnetization plateau at half-saturation. Our results can be verified in experiments with vanadium oxides of the type $PbVO_3$. Assuming[19] that $J_1 \sim 70$–100 K (and J_2, J_C inside the paramagnetic phase), one gets $T_0 \sim 20$–30 K and $h_M \sim 25$–35 T. The magnetization plateau should become apparent for $h \sim 100$–200 T.

Acknowledgments. We thank J. Dukelsky for illuminating discussions. L.I. was supported by DOE via Grant No. DE-FG02-08ER46492.

[1] *Introduction to Frustrated Magnetism: Materials, Experiments, Theory*, edited by C. Lacroix, P. Mendels, and F. Mila (Springer, Berlin, 2011).

[2] S. Ladak, D. E. Read, G. K. Perkins, L. F. Cohen, and W. R. Branford, Nat. Phys. **6**, 359 (2010).

[3] S. R. Giblin, S. T. Bramwell, P. C. W. Holdsworth, D. Prabhakaran, and I. Terry, Nat. Phys. **7**, 252 (2011).

[4] M. Takigawa and F. Mila, in *Introduction to Frustrated Magnetism: Materials, Experiments, Theory* (Ref. 1), Chap. 10.

[5] L. Isaev, G. Ortiz, and J. Dukelsky, Phys. Rev. Lett. **103**, 177201 (2009).

[6] L. Balents, Nature (London) **464**, 199 (2010).

[7] K. Matan, T. Ono, Y. Fukumoto, T. J. Sato, J. Yamaura, M. Yano, K. Morita, and H. Tanaka, Nat. Phys. **6**, 865 (2010).

[8] A. M. Läuchli, in *Introduction to Frustrated Magnetism: Materials, Experiments, Theory* (Ref. 1), Chap. 18.

[9] *Quantum Magnetism*, edited by U. Shollwöck, J. Richter, F. J. J. Farnel, and R. F. Bishop (Springer, Berlin, 2004).

[10] L. Isaev, G. Ortiz, and J. Dukelsky, Phys. Rev. B **79**, 024409 (2009).

[11] J. P. Blaizot and G. Ripka, *Quantum Theory of Finite Systems* (The MIT Press, Cambridge, MA, 1986).

[12] D. Schmalfuß, R. Darradi, J. Richter, J. Schulenburg, and D. Ihle, Phys. Rev. Lett. **97**, 157201 (2006).

[13] W. Nunes, J. R. Viana, and J. R. de Sousa, J. Stat. Mech. (2011) P05016.

[14] O. Rojas, C. J. Hamer, and J. Oitmaa, J. Phys.: Condens. Matter **23**, 416001 (2011).

[15]P. Thalmeier, B. Schmidt, V. Yushankhai, and T. Takimoto, Acta Phys. Pol., A **115**, 53 (2009).

[16]P. Thalmeier, M. E. Zhitomirsky, B. Schmidt, and N. Shannon, Phys. Rev. B **77**, 104441 (2008).

[17]B. Schmidt, P. Thalmeier, and N. Shannon, J. Phys.: Conf. Ser. **145**, 012054 (2009).

[18]A. Bombardi, J. Rodriguez-Carvajal, S. DiMatteo, F. de Bergevin, L. Paolasini, P. Carretta, P. Millet, and R. Caciuffo, Phys. Rev. Lett. **93**, 027202 (2004).

[19]A. A. Tsirlin, A. A. Belik, R. V. Shpanchenko, E. V. Antipov, E. Takayama-Muromachi, and H. Rosner, Phys. Rev. B **77**, 092402 (2008).

[20]G. Misguich and C. Lhuillier in *Frustrated Spin Systems*, edited by H. T. Diep (World Scientific, Singapore, 2004).

[21]The character of the Néel-paramagnetic phase transition is a subtle issue. While this phase transition is continuous in the present study, due to the real-space nature of the THMF method (which involves explicit translational symmetry breaking), we cannot rule out the possibility of a weakly first-order transition in the *translationally invariant* J_1-J_2-J_C model. A more complete discussion is presented in Ref. 10.

[22]M. E. Zhitomirsky, A. Honecker, and O. A. Petrenko, Phys. Rev. Lett. **85**, 3269 (2000).

[23]G. L. Bir and G. E. Pikus, *Symmetry and Strain-Induced Effects in Semiconductors* (Wiley, New York, 1974).

[24]N. D. Mermin and H. Wagner, Phys. Rev. Lett. **17**, 1133 (1966).

[25]P. Chandra, P. Coleman, and A. I. Larkin, Phys. Rev. Lett. **64**, 88 (1990).

[26]R. Darradi, O. Derzhko, R. Zinke, J. Schulenburg, S. E. Kruger, and J. Richter, Phys. Rev. B **78**, 214415 (2008).

[27]J. B. Fouet, M. Mambrini, P. Sindzingre, and C. Lhuillier, Phys. Rev. B **67**, 054411 (2003).

[28]C. Holm and W. Janke, Nucl. Phys. B **30**, 846 (1993).

[29]P. Sengupta, A. W. Sandvik, and R. R. P. Singh, Phys. Rev. B **68**, 094423 (2003).